

Scattering and absorption sections of Schwarzschild-anti de Sitter with quintessence

L. A. López,^{*} Omar Pedraza,[†] V. E. Ceron,[‡] and Valeria Ramírez[§]

*Área Académica de Matemáticas y Física,
UAEH, Carretera Pachuca-Tulancingo Km. 4.5,
C P. 42184, Mineral de la Reforma, Hidalgo, México.*

Abstract

In this paper, we study the Schwarzschild-anti de Sitter black hole surrounded by quintessence. The critical values of the cosmological constant and the normalization factor are obtained. We described the event horizons and the extremal condition of the black hole surrounded by quintessence. Also, the effects of quintessence on the classical and semiclassical scattering cross-sections have been estimated. The absorption section is studied with the sinc approximation in the eikonal limit. This study considers the quintessence state parameter in the particular cases $\omega = -2/3$ and $\omega = -1/2$.

PACS numbers: 04.20.-q, 04.70.-s, 04.30.Nk, 11.80.-m

^{*}Electronic address: lalopez@uaeh.edu.mx

[†]Electronic address: omarp@uaeh.edu.mx

[‡]Electronic address: vceron@uaeh.edu.mx

[§]Electronic address: ra323273@uaeh.edu.mx

I. INTRODUCTION

The universe contains a high percentage of dark energy, and this energy is responsible for the accelerated expansion of the universe. Also, the cosmological constant can play a very considerable role in the dynamics of the universe because it is the first and simplest explanation of dark energy [1].

The evidence that the universe contains black holes (BH) of different solar masses [2], has led to various studies and observations. In this sense, studying the consequences of the black holes coexistence with other types of matter or energy is essential.

There are alternative models as candidates for dark energy, based on a scalar fields as are quintessence [3], phantom [4], K-essence [5] among others.

Applying the ideas of Kiselev (2003) [6] that presented a new static spherically symmetric exact solutions of the Einstein equations for quintessential matter surrounding a BH, different investigations have emerged. For example; the null geodesics for Schwarzschild surrounded by quintessence in [7] is addressed as well as Reissner-Nordström surrounded by quintessence in [8] also the thermodynamics of the black holes with quintessence are studied in [9] and Hayward black hole surrounded by quintessence in [10].

Recently the scattering and absorption sections of black holes surrounded by quintessence have been addressed in [11]. The geodesic structure of massless particles of the Schwarzschild-anti de Sitter BH with quintessence is studied in [12] also the dynamics of neutral and charged particles around the AdS Schwarzschild black hole surrounded by quintessence is discussed in [13]. We shall combine some of these ideas for our purposes below.

In the present paper, we propose to study the scattering and absorption sections of Schwarzschild-anti de Sitter black hole surrounded by quintessence, because a way to explore the physics of a BH is to analyze the absorption and scattering of the test fields around them.

The paper is organized as follows: In Sec. II the Schwarzschild-anti de Sitter black hole surrounded by quintessence is presented, the critical values of cosmological constant and normalization factor are shown, also are analysed the event horizons and the case extremal. In the section III, the expressions for the classical and semi-classical scattering sections are presented. IV we analyzed the sections for $\omega = -2/3$ and $\omega = -1/2$ in detail. Section V taking the same values the adsorption section is obtained by sinc approximation. Finally,

conclusions are given in the last section.

II. SCHWARZSCHILD-ANTI DE SITTER SURROUNDED BY QUINTESSENCE

When the cosmological constant is included in the Einstein equations, one obtain solutions that represent black holes with various asymptotic. Among them, asymptotically anti-de Sitter black holes as Schwarzschild-anti de Sitter. The space anti-de Sitter have attracted a lot of attention recently because the AdS/CFT correspondence [14], which is a correspondence between a gravitation theory and a quantum field theory, may be applied to strongly coupled systems. The timelike property of the AdS boundary is other characteristic interesting as compared to other asymptotic space-times.

Then using the ideas of Kiselev [6] that proposed solutions static and spherically symmetric that describe Black holes surrounded by quintessence. The solution of the Schwarzschild-anti de Sitter black hole surrounded by quintessence (Sch-aBH- ω) is written as

$$ds^2 = -f(r)dt^2 + \frac{dr^2}{f(r)} + r^2 d\theta^2 + r^2 \sin^2 \theta d\phi^2, \quad (1)$$

with

$$f(r) = 1 - \frac{2M}{r} - \frac{\Lambda r^2}{3} - \frac{C}{r^{3\omega+1}}. \quad (2)$$

Where M is the mass of the black hole and Λ is the cosmological constant. The magnitude of ω witch is the ratio of pressure to energy density takes values between $-1 < \omega < -1/3$. The density of quintessence is always positive and given by:

$$\rho = -\frac{C}{2} \frac{3\omega}{r^{3(\omega+1)}}, \quad (3)$$

where the constant C is a positive normalization factor. For $\Lambda = 0$ we obtain the Schwarzschild black hole surrounded by quintessence that in [7] is studied. In [12] the null geodesics and the kinds of orbits are analized considering the particular case $\omega = -2/3$.

The event horizons of the space-time (1) are defined by the divergence of the function metric g_{rr} that corresponds the positive roots of the function metric $f(r)$, for this analysis and the consequent analyses, we express radial distance and the parameter C in units of mass as $r \rightarrow r/M$, $C \rightarrow C/M^b$, in the case of the cosmological constant we consider $\Lambda \rightarrow \Lambda M^2$,

with $b = 3\omega + 1$, then the event horizons are the roots of $3Cr + 6r^b - 3r^{1+b} + r^{3+b}\Lambda = 0$, the number of horizons depends entirely on the choice of the values of parameters ω , C and Λ .

Of the condition $f(r) = 0$ we parametrize Λ as a function of r and C as;

$$\Lambda(r, C) = 3^{-(3+b)}(r^{1+b} - 2r^b - Cr). \quad (4)$$

The cosmological constant has extremal for a $C(r)$ given by;

$$C(r) = \frac{2(r-3)r^{b-1}}{b+2}. \quad (5)$$

$C(r)$ has extremal in certain r_{crit} , performing an analysis we obtain;

$$r_{crit} = \frac{3(b-1)}{b}. \quad (6)$$

So, the critical value of the quintessential parameter $C_{crit} = C(r_{crit})$ and the corresponding cosmological constant ($\Lambda(C_{crit}, r_{crit}) = \Lambda_{crit}$) are given by

$$C_{crit} = -\frac{2(3-3/b)^b}{-2+b+b^2}, \quad \Lambda_{crit} = \frac{b^3}{18-27b+9b^3}. \quad (7)$$

In terms of ω , Eq. (7) can be expressed as

$$C_{crit} = -\frac{2(9\omega)^{3\omega}}{(1+\omega)(1+3\omega)^{1+3\omega}}, \quad \Lambda_{crit} = \frac{(1+3\omega)^3}{243\omega^2(1+\omega)}. \quad (8)$$

The behavior of the critical values Λ_{crit} and C_{crit} are shown in figure (1). The Sch-aBH- ω has horizons for values of $\Lambda_{crit} \leq \Lambda$ and $C \leq C_{crit}$. In Fig (1) shows that as ω increases, C_{crit} decreases and presents a minimum (in $\omega \approx -0.796807$) then increases as ω increases.

On the other hand, when $\omega \rightarrow -1/3$, we observed that $\Lambda_{crit} \rightarrow 0$ (see Fig 1) means that a Schwarzschild black hole surrounded by quintessence is formed.

In summary for $\Lambda_{crit} \leq \Lambda \leq 0$ and $0 < C \leq C_{crit}$ the Sch-aBH- ω can represent a black holes with different horizons r_{in} , r_{out} and r_ω (quintessence horizon).

The Sch-aBH- ω extremal can be obtained when the conditions $f(r) = 0$ and $\frac{d}{dr}f(r) = 0$ are satisfied simultaneously. Introducing the $\Lambda(r, C)$ of (4) in $\frac{d}{dr}f(r) = 0$, we obtained the condition $(2Cr + bCr + 6r^b - 2r^{1+b})r^{-2-b} = 0$ that can have two real roots denoted by r_+ and r_- .

If we will focus on the particular case of $\omega = -2/3$ the roots r_+ and r_- are given by;

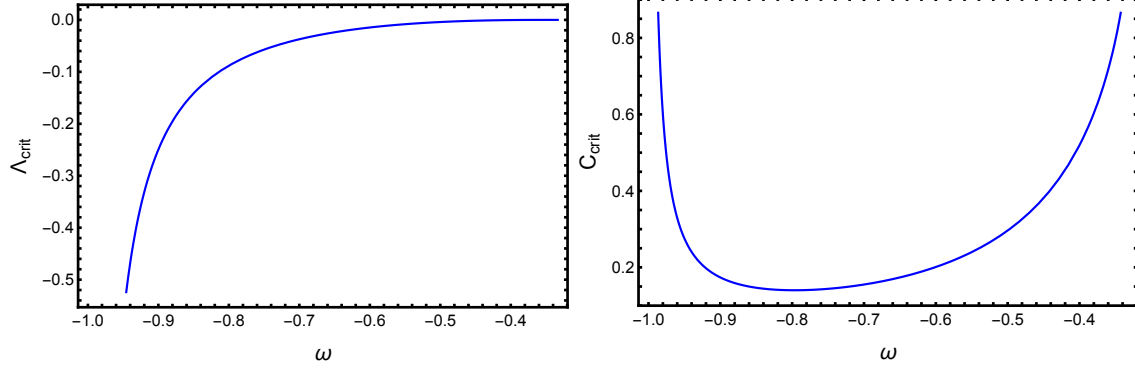


FIG. 1: The figures show the behavior of Λ_{crit} and C_{crit} in function of ω in the range $-1 < \omega < -1/3$. Notice that as ω grows, Λ_{crit} also grows on the other hand C_{crit} has a minimum for $\omega \approx -0.796807$.

$$r_{\pm} = \frac{1 \pm \sqrt{1 - 6C}}{C}. \quad (9)$$

In figure (2) the behavior of Λ as function of C is shown for $\omega = -2/3$. In the regions I and III, the Sch-aBH- ω have one horizon, while in the region II there are three horizons. The boundary ($\Lambda(C, r_-)$) of regions I and II as well as the boundary of regions II and III ($\Lambda(C, r_+)$) represents the extremal of Sch-aBH- ω .

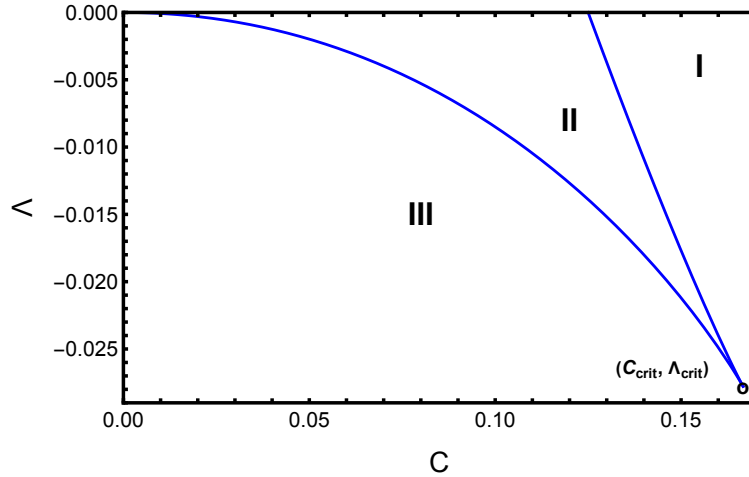


FIG. 2: The behavior of Λ as a function of C is shown for $\omega = -2/3$. The regions I, II and III contain the values of Λ and C so that Sch-aBH- ω has one horizon (regions I and III), three horizons (region II), and the boundary of the regions are the values that represent the extreme case.

Depending on the values of the parameters Λ and C the number of the horizons may decrease from three to one, the cosmological horizon r_ω (quintessence horizon) never vanishes, then in this case we say that the Sch-aBH- ω describes a naked singularity.

The development carried out for $\omega = -2/3$ can be applied for different values of ω , however, the analysis must be numeric. The region II, where Sch-aBH- ω has three horizons, is modified as shown in the figure (3) $II_{\omega=-2/3} > II_{\omega=-1/2} > II_{\omega=-4/9}$.

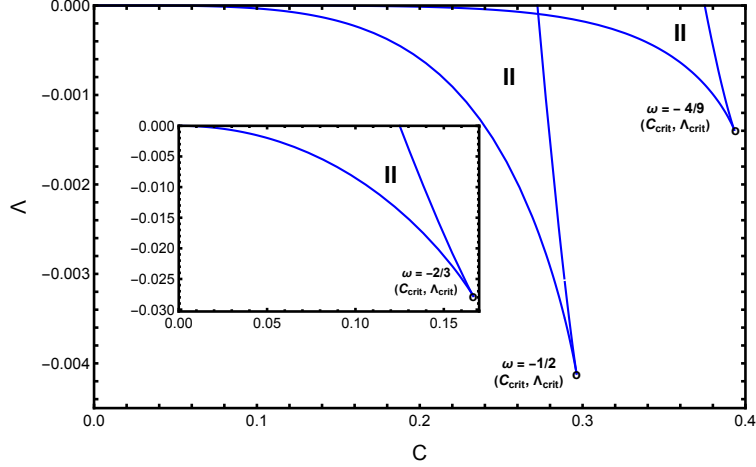


FIG. 3: The figure shows Λ as a function of C for different ω ; also, the critical values are shown. From the figure, we can see that for region II the values of Λ for $\omega = -2/3$ are greater compared to $\omega = -4/9$.

The conditions for some values of ω are summarized in Table I that shows the values of Λ_{crit} and C_{crit} , it is clear how the factor ω modifies the behavior of the horizons of Sch-aBH- ω .

ω	$-4/9$	$-1/2$	$-5/9$	$-2/3$	$-7/9$	$-8/9$
Λ_{crit}	$-1/720$	$-1/243$	$-2/225$	$-1/36$	$-32/441$	$-125/576$
C_{crit}	0.3931	0.2962	0.2348	0.1666	0.140907	0.16473

TABLE I: Critical values of the Λ and C for different ω

In all cases $\omega = -2/3$, $\omega = -4/9$ and $\omega = -1/2$, the inner and out horizons merge into a single horizon $r_{in} = r_{out}$, in boundary of regions I and II. When $r_{out} = r_\omega$ the boundary of regions II and III are considered. Finally if all horizons merge into a single horizon, and the Kiselev black holes is known as a super-extremal black hole.

III. CLASSICAL AND SEMI-CLASSICAL SCATTERING CROSS SECTIONS

To obtain the scattering cross section, a procedure used is the study of geodesics for the classical approximation. The geodesic analysis is important because at very high frequencies the wave propagates along null geodesics[15].

The test particles propagate along of null geodesics are described by the Lagrangian density $\mathcal{L} = -\frac{1}{2}\dot{x}^\mu\dot{x}_\mu = 0$, where "dot" denotes the derivative with respect to the affine parameter τ .

We restrict the geodesic motion to the plane $\theta = \pi/2$ and solving for \dot{r}^2 , we obtain $\dot{r}^2 = E^2 - V_{eff}$, where $V_{eff} = f(r)\frac{l^2}{r^2}$. The energy $E = \frac{\partial\mathcal{L}}{\partial t}$ and the angular momentum $L = -\frac{\partial\mathcal{L}}{\partial\phi}$ of a test particle are conserved. As the impact parameter is defined as $\hat{b} = L/E$ is possible to obtain the impact parameter (\hat{b}_c) associated with the critical orbits, for any $\hat{b} > \hat{b}_c$ there is no scattering.

If we defined $u = 1/r$ and consider $\dot{r}^2 = E^2 - V_{eff}$, we can obtained the expression;

$$\left(\frac{du}{d\phi}\right)^2 = \frac{1}{\hat{b}^2} - f(1/u)u^2. \quad (10)$$

Differentiating (10) with respect to ϕ , we obtained

$$\frac{d^2u}{d\phi^2} = -\frac{u^2}{2} \frac{df(1/u)}{du} - uf(1/u). \quad (11)$$

if we consider $\frac{d^2u}{d\phi^2} = 0$ the positive root corresponds to the radius of the critical orbit for null geodesic u_c and substituting in (10), we obtained the critical impact parameter \hat{b}_c .

In the case of geodesics coming from the infinity to a turning point u_0 , the deflection angle is given by;

$$\Theta(\hat{b}) = 2\phi(\hat{b}) - \pi, \quad (12)$$

where

$$\phi = \int_0^{u_0} du \left(\frac{1}{\hat{b}^2} - u^2 f(1/u) \right)^{-1/2}. \quad (13)$$

The impact parameter $\hat{b}(\Theta)$, associated with the classical scattering cross section is given by;

$$\frac{d\sigma}{d\Omega} = \frac{1}{\sin\Theta} \sum \hat{b}(\Theta) \left| \frac{d\hat{b}(\Theta)}{d\Theta} \right|. \quad (14)$$

Now when we consider partial waves in the scattering phenomenon, it is necessary to consider the interference that occurs between partial waves with different angular momenta. This situation is not considered by the classical scattering cross-section (14). The approximate method that considers the interference of the waves for low angles and high-frequency scalar plane waves ($\omega \gg 1$) is the semi-classical approach (Glory scattering) [16]. The glory approximation of the scalar scattering cross-section by spherically symmetric Black Holes is given by;

$$\frac{d\sigma_g}{d\Omega} = 2\pi w \hat{b}_g^2 \left| \frac{d\hat{b}}{d\Theta} \right|_{\Theta=\pi} J_{2s}^2(w \hat{b}_g \sin \Theta), \quad (15)$$

with w as the wave frequency. J_{2s}^2 stands for the Bessel function of first kind of order $2s$ where s represents the spin, $s = 0$ for scalar waves. The impact parameter of the reflected waves ($\theta \sim \pi$) is denoted by \hat{b}_g . As a semi-classical approximation, it is valid for $Mw \gg 1$ (M the mass of the BH).

IV. CLASSICAL AND SEMI-CLASSICAL SCATTERING CROSS-SECTIONS FOR $\omega = -2/3$ AND $\omega = -1/2$

In this section, the classical and semi-classical scattering cross-sections are obtained for Sch-aBH- ω . We analyse and compare the differences that can be similar but not identical. To carry out the analyzing scattering cross-section, we consider $\omega = -2/3$ and $\omega = -1/2$.

The u_c (radius r_c) of the critical orbit for null geodesic is obtained of the equation (16);

$$2 - (2 + b)Cu_c^b - 6u_c = 0, \quad (16)$$

and the critical impact parameter \hat{b}_c is given by;

$$M^{-2}\hat{b}_c^2 = \frac{3}{3u_c^2 - 6u_c^3 - 3Cu_c^{2+b} - \Lambda}, \quad (17)$$

u_c is reported in [12] for the case of $\omega = -2/3$ ($u_c = (1 + \sqrt{1 - 6C})/6$). Now for case $\omega = -1/2$, u_c is given by;

$$u_c = \frac{27A^{1/3}C^2}{-64 + 64i\sqrt{3} + 16A^{1/3} - A^{2/3} - i\sqrt{3}A^{2/3} + 648C^2 - 648i\sqrt{3}C^2}, \quad (18)$$

Where $A = 512 - 7776C^2 + 19683C^4 + 729\sqrt{729C^8 - 64C^6}$. It is possible to observe that the different u_c do not depend on the cosmological constant explicitly. Then the maximum of the effective potential is generated by C . The figure (4) the behavior of the critical impact parameter is shown for $\omega = -2/3$ and $\omega = -1/2$, in both cases \hat{b}_c increases as C increases and in the limit $C \rightarrow 0$ both impact parameters tend to $27/(1 - 9\Lambda)$.

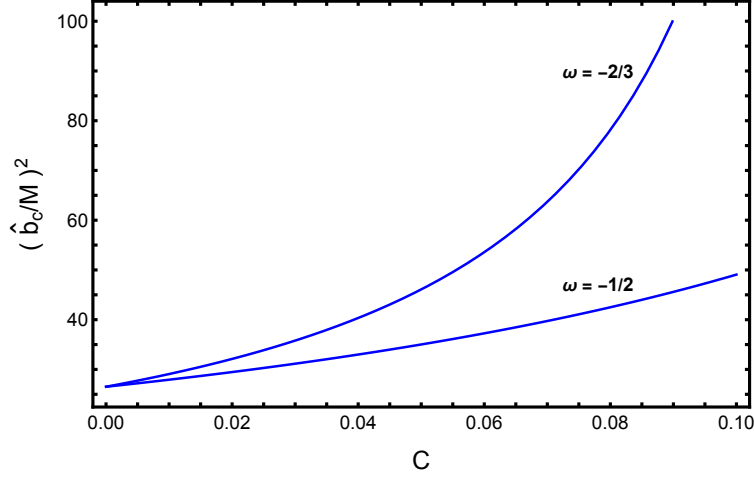


FIG. 4: The behavior of $(b_c/M)^2$ as function of C is shown for different ω and $\Lambda = -0.002$, the relative magnitudes of the critical impact parameters are $(\hat{b}_c)_{-2/3} > (\hat{b}_c)_{-1/2}$

In some cases of ω allow a relatively simple treatment of the properties of the geodesic equation of motion (10), then in order to analyze the geodesic equation we consider $\omega = -2/3$, that it can be written as;

$$\left(\frac{du}{d\phi}\right)^2 = 2(u - u_1)(u - u_2)(u - u_3). \quad (19)$$

Where u_i are the roots of (10) given by;

$$u_1 = \frac{(1 - \sqrt{3}i)\left(\frac{3C}{2} - \frac{1}{4}\right)}{2^{3/2}3\Delta} - \frac{(1 + \sqrt{3}i)\Delta}{2^{1/3}6} + \frac{1}{6}, \quad (20)$$

$$u_2 = \frac{(1 + \sqrt{3}i)\left(\frac{3C}{2} - \frac{1}{4}\right)}{2^{3/2}3\Delta} - \frac{(1 - \sqrt{3}i)\Delta}{2^{1/3}6} + \frac{1}{6}, \quad (21)$$

$$u_3 = -\frac{2^{1/3}\left(\frac{3C}{2} - \frac{1}{4}\right)}{3\Delta} + \frac{\Delta}{2^{1/3}3} + \frac{1}{6}, \quad (22)$$

$$\Delta = \left(\sqrt{\delta + 4\left(\frac{3C}{2} - \frac{1}{4}\right)^3} - \frac{27}{2\hat{b}^2 M^{-2}} - \frac{9C}{4} + \frac{1}{4} - \frac{9\Lambda}{2}\right)^{1/3}, \quad (23)$$

$$\delta = \left(-\frac{27}{2b^2} - \frac{9C}{4} + \frac{1}{4} - \frac{9\Lambda}{2} \right)^2, \quad (24)$$

and $u_1 < u_2 < u_3$. Then (13) take the form;

$$\int_0^u \frac{du}{\sqrt{2(u-u_1)(u-u_2)(u-u_3)}} = -\frac{2}{\sqrt{2(u_2-u_1)}} F(\xi, y), \quad (25)$$

with, the incomplete elliptic integral

$$F(\xi, y) = \int_0^{\sin \xi} \frac{dx}{\sqrt{1-x^2}\sqrt{1-x^2y^2}}, \quad (26)$$

where,

$$\xi = \arcsin \sqrt{\frac{u_2-u_1}{u-u_1}}, \quad y = \sqrt{\frac{u_1-u_3}{u_1-u_2}}. \quad (27)$$

Finally we obtain.

$$\phi = -\frac{2}{\sqrt{2M(u_2-u_1)}} F(\xi, y) + \phi_0. \quad (28)$$

Solving (28) numerically with appropriate boundary conditions, one can obtain the null geodesic followed by Sch-aBH- ω . In the case of $\omega = -1/2$ the analytic computation of (28) is almost impossible, then the solution is numerically obtained.

The corresponding motion of geodesics is given in the figure (5), and show the scattering of geodesics, as $r_\omega > r_{out}$ then the movement of the null geodesics can be located within the quintessence horizon (apparent horizon), but if it passes within the horizon $r = r_{out}$, the geodesics fall into the black hole. The above is considered for obtain the Classical and semi-classical scattering cross-sections.

In figure (6), the classical cross-sections for Sch-aBH- ω are compared consider different values of Λ and C in the case that Sch-aBH- ω has three horizons. It is possible to note that in both cases ($\omega = -2/3$ and $\omega = -1/2$) there is no significant difference between in the case of the classical scattering cross-section for small and large angles.

Comparing the scattering cross-sections from Sch-aBH- ω and Schwarzschild black hole surrounded by quintessence ($\Lambda = 0$), we observe that the cross-section of Schwarzschild black hole surrounded is greater than the one from Sch-aBH- ω for both cases $\omega = -2/3$ and $\omega = -1/2$.

The semi-classical scattering differential cross-sections for Sch-aBH- ω with $\omega = -2/3$ and $\omega = -1/2$ are shown in the figure (7). We can be observed that in the case of Sch-aBH- ω the

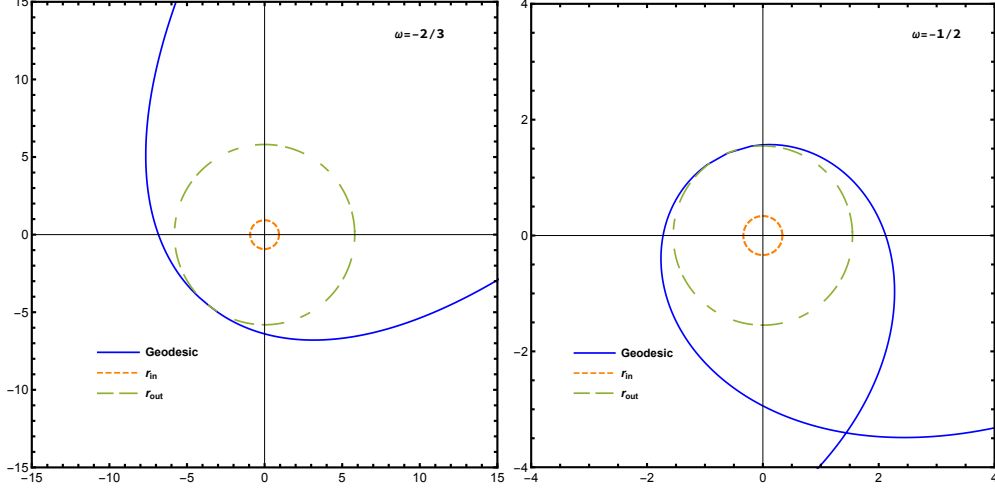


FIG. 5: The figures shown the behavior of geodesics approaching a Sch-aBH- ω from infinity, for $\omega = -2/3$ and $\omega = -1/2$.

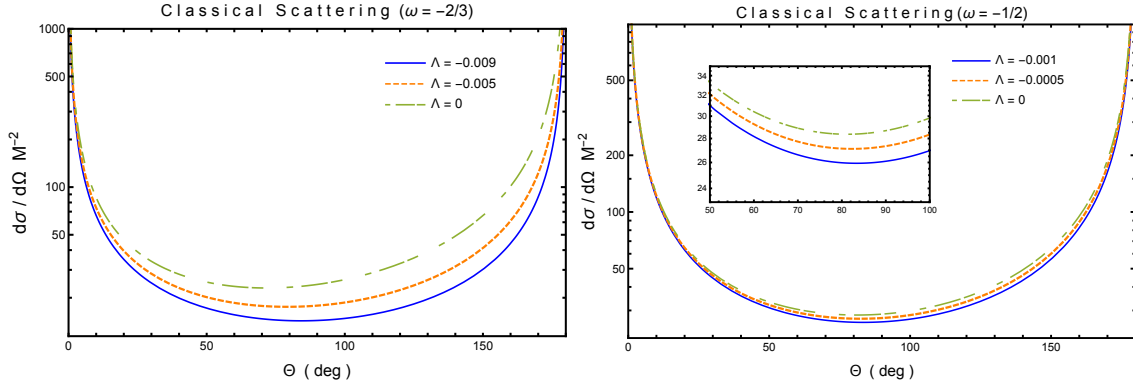


FIG. 6: The behavior of classical scattering cross-section is shown varying the value of Λ , in the first panel, we plot the cross-section for $\omega = -2/3$ with $C = 0.12$ and the second panel, the cross-section is plotted for $\omega = -1/2$ and $C = 0.25$ in the small box the difference between the cross-sections for $\omega = -1/2$ are shown.

scattering section is highly similar to Schwarzschild black hole surrounded by quintessence ($\Lambda = 0$) section. However, with $\omega = -2/3$, the differences are more noticeable.

Regarding the cross-sections, it is possible to mention that when we vary the normalization factor C , the behavior of cross-sections is similar to that in the case when Λ changes.

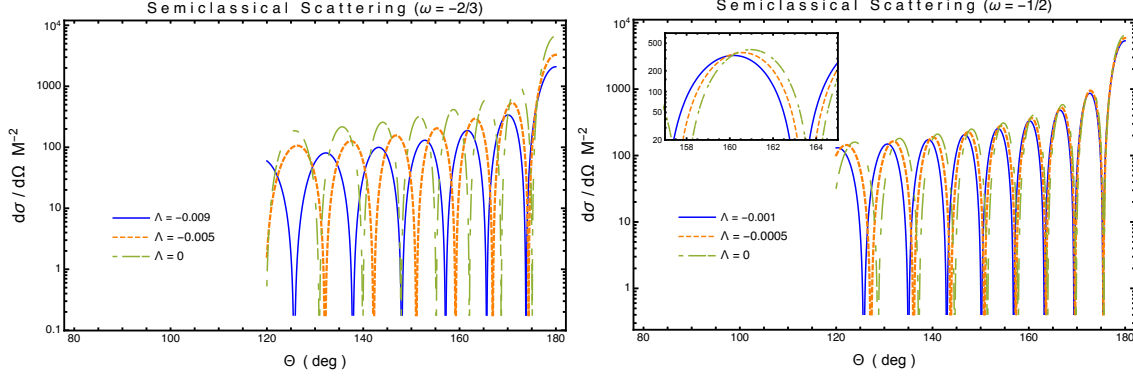


FIG. 7: The behavior of semi-classical scattering cross-section is shown varying the value of the cosmological constant Λ , in the first panel, we plot the for $\omega = -2/3$ with $C = 0.12$ and the second panel, the semi-classical cross-section is plotted for $\omega = -1/2$ and $C = 0.25$ in the small box the difference between the semi-classical cross-sections for $\omega = -1/2$ are shown, in both cases we consider $Mw = 2$.

V. ABSORPTION CROSS SECTION

In the approximation of low frequencies, the absorption cross-section by spherically symmetric Black Holes equals the BH horizon area [17].

In the approximation of high frequencies, the absorption cross section can be considered the classical capture cross -section of the null geodesics in massless scalar waves. In this limit the absorption cross section is also called geometric cross-section $\sigma_{geo} = \pi \hat{b}_c^2$.

In [18] the author showed that in the case of high frequencies (eikonal limit) the oscillatory part of the absorption cross-section can be written in terms of the parameters of the unstable null circular orbits.

Then the absorption cross section in the eikonal limit is defined by ;

$$\sigma_{osc} = -4\pi \frac{\lambda \hat{b}_c^2}{w} e^{-\pi \lambda \hat{b}_c} \sin\left(\frac{2\pi w}{\Omega_c}\right), \quad (29)$$

where λ is the Lyapunov [19] exponent given by;

$$\lambda^2 = \frac{f(r_c)}{2r_c^2} \left[2f(r_c) - r_c^2 f''(r_c) \right], \quad (30)$$

r_c , the radius of the unstable null circular orbit and b_c is the critical impact parameter. while the orbital angular velocity is ;

$$\Omega_c = \sqrt{\frac{f_c}{r_c^2}}. \quad (31)$$

Then the absorption cross-section in the limit of high frequencies can write is proportional to the sum of σ_{osc} and σ_{geo} (the sinc approximation)

$$\sigma_{sinc} \approx \sigma_{geo} + \sigma_{osc}. \quad (32)$$

A. Absorption cross-section with $\omega = -2/3$ and $\omega = -1/2$

In this subsection, the absorption cross-sections in the sinc approximation are obtained for Sch-aBH- ω . We analyse and compare the differences that can be similar but not identical.

The Lyapunov exponent for $\omega = -2/3$ is given by;

$$M^2 \lambda_{\omega=-2/3}^2 = \frac{(Cr_c - 1)(6 - 3r_c + 3Cr_c^2 + r_c^3 \Lambda)}{3r_c^3}, \quad (33)$$

with r_c is reported in [12] as previously mentioned and the Lyapunov exponent for $\omega = -1/2$ is given by;

$$M^2 \lambda_{\omega=-1/2}^2 = \frac{(9C\sqrt{r_c} - 8)(6 - 3r_c + 3Cr_c^{3/2} + r_c^3 \Lambda)}{24r_c^3}, \quad (34)$$

the r_c for the case $\omega = -1/2$ were obtained in (18)

The absorption cross-sections for $\omega = -2/3$ and $\omega = -1/2$ are plotted in Figure (8), respectively in the case of the sinc approximation. It is obvious that the amplitude of absorption cross-section tends to zero as wM increases. It also shows that the difference of the curves is numerically significant with respect to their amplitude with larger values of wM in both cases.

Moreover, for each value ω , is possible mention that $\sigma_{-1/2} > \sigma_{-2/3}$, also the corresponding absorption cross-section starts from zero, reaches a maximum value σ_{Abs} , and decreases asymptotically. Finally, when we consider $\omega = -1/2$, the behavior shows that differences are present in lesser scale than with $\omega = -2/3$

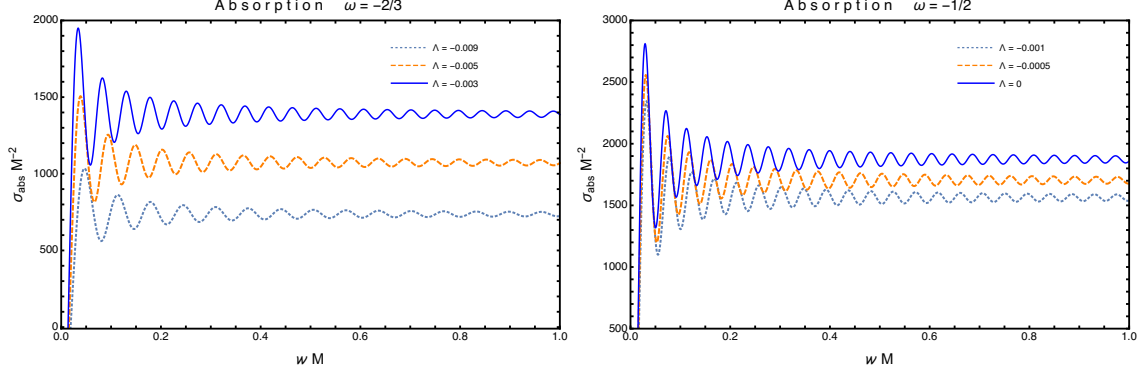


FIG. 8: The behavior of absorption cross section in the sinc limit is shown varying the value of the cosmological constant Λ , in the first panel, we plot the absorption cross section for $\omega = -2/3$ with $C = 0.12$ and the second panel, the absorption cross-section is plotted for $\omega = -1/2$ and $C = 0.25$

VI. CONCLUSIONS

In this paper, we shown how the scattering and absorption sections are modified by considering the effects quintessence in the Schwarzschild-anti de Sitter black hole.

First, we presented the critical values of the C_{crit} (normalization factor) and cosmological constant (Λ) in term of ω , when $\Lambda_{crit} \leq \Lambda$ and $C \leq C_{crit}$ the solution of Schwarzschild-anti de Sitter surrounded by quintessence (Sch-aBH- ω) has one, two, or three horizons. The regions where the Sch-aBH- ω has one, two, or three horizons are analyzed in the particular cases $\omega = -2/3, -1/2, -4/9$ and we see that the behavior is the same for all values. Also the extremal BH is studied. When $\omega \rightarrow -1/3$ we observed that a Schwarzschild black hole surrounded by quintessence is formed and C_{crit} presents a minimum in $\omega \approx -0.796807$.

The classical and semi-classical scattering cross-sections are compared for different values of the cosmological constant, and we fixed $\omega = -2/3$ and $\omega = -1/2$. For the numerical analysing of cross-sections we consider the ranges of the cosmological constant and the normalization factor where the Sch-aBH- ω has three horizons. We observe that the classical and semi-classical scattering cross-sections for Schwarzschild are greater than Schwarzschild-anti de Sitter, both surrounded by quintessence. For $\omega = -2/3$, the differences between the cross-sections are more noticeable because the impact parameters to $\omega = -2/3$ are more significant than to $\omega = -1/2$.

For the absorption cross-section the sinc approximation is used, so that the absorption

section is given in function of the Lyapunov exponent and the impact parameter for a null circular unstable geodesic. The Schwarzschild surrounded by quintessence is more larger than the absorption cross-section of Schwarzschild-anti de Sitter surrounded by quintessence and both decreases asymptotically. In this case, the absorption cross-section is larger for $\omega = -1/2$ than for $\omega = -2/3$.

ACKNOWLEDGMENT

The authors acknowledge the financial support from PROMEP project UAEH-CA-108 and SNI-CONACYT, México.

-
- [1] T. Padmanabhan. Accelerated expansion of the universe driven by tachyonic matter. *Phys. Rev. D*, 66:021301, 2002.
 - [2] Mitchell C. Begelman. Evidence for black holes. *Science*, 300(5627):1898–1903, 2003.
 - [3] S Capozziello, V F Cardone, E Piedipalumbo, and C Rubano. Dark energy exponential potential models as curvature quintessence. *Classical and Quantum Gravity*, 23(4):1205–1216, feb 2006.
 - [4] Luis P. Chimento and Ruth Lazkoz. Constructing phantom cosmologies from standard scalar field universes. *Phys. Rev. Lett.*, 91:211301, Nov 2003.
 - [5] C. Armendariz-Picon, V. Mukhanov, and Paul J. Steinhardt. Dynamical solution to the problem of a small cosmological constant and late-time cosmic acceleration. *Phys. Rev. Lett.*, 85:4438–4441, Nov 2000.
 - [6] V.V. Kiselev. Quintessence and black holes. *Class. Quant. Grav.*, 20:1187–1198, 2003.
 - [7] Sharmanthie Fernando. Schwarzschild black hole surrounded by quintessence: Null geodesics. *Gen. Rel. Grav.*, 44:1857–1879, 2012.
 - [8] B. Malakolkalami and K. Ghaderi. The null geodesics of the Reissner–Nordström black hole surrounded by quintessence. *Mod. Phys. Lett. A*, 30(10):1550049, 2015.
 - [9] K. Ghaderi and B. Malakolkalami. Effects of quintessence on thermodynamics of the black holes. *Astrophys. Space Sci.*, 361(5):161, 2016.

- [10] Omar Pedraza, L. A. López, R. Arceo, and I. Cabrera-Munguia. Geodesics of Hayward black hole surrounded by quintessence. *Gen. Rel. Grav.*, 53(3):24, 2021.
- [11] L. A. López and Omar Pedraza. Effects of quintessence on scattering and absorption sections of black holes. 3 2021.
- [12] B. Malakolkalami and K. Ghaderi. Schwarzschild-anti de Sitter black hole with quintessence. *Astrophys. Space Sci.*, 357(2):112, 2015.
- [13] Amir Sultan Khan, Farhad Ali, and Israr Ali Khan. Dynamics of a particle around AdS Schwarzschild black hole environed by quintessence. *Can. J. Phys.*, 99(5):329–339, 2021.
- [14] S. S. Gubser, Igor R. Klebanov, and Alexander M. Polyakov. Gauge theory correlators from noncritical string theory. *Phys. Lett. B*, 428:105–114, 1998.
- [15] P A Collins, R Delbourgo, and R M Williams. On the elastic schwarzschild scattering cross section. *Journal of Physics A: Mathematical, Nuclear and General*, 6(2):161–169, feb 1973.
- [16] Richard A. Matzner, Cécile DeWitte-Morette, Bruce Nelson, and Tian-Rong Zhang. Glory scattering by black holes. *Phys. Rev. D*, 31:1869–1878, Apr 1985.
- [17] Atsushi Higuchi. Low frequency scalar absorption cross-sections for stationary black holes. *Class. Quant. Grav.*, 18:L139, 2001. [Addendum: *Class.Quant.Grav.* 19, 599 (2002)].
- [18] Yves Décanini, Gilles Esposito-Farèse, and Antoine Folacci. Universality of high-energy absorption cross sections for black holes. *Phys. Rev. D*, 83:044032, Feb 2011.
- [19] V. Cardoso, A. S. Miranda, E. Berti, H. Witek, and V. T. Zanchin. Geodesic stability, Lyapunov exponents and quasinormal modes. *Phys. Rev.*, D79:064016, 2009.